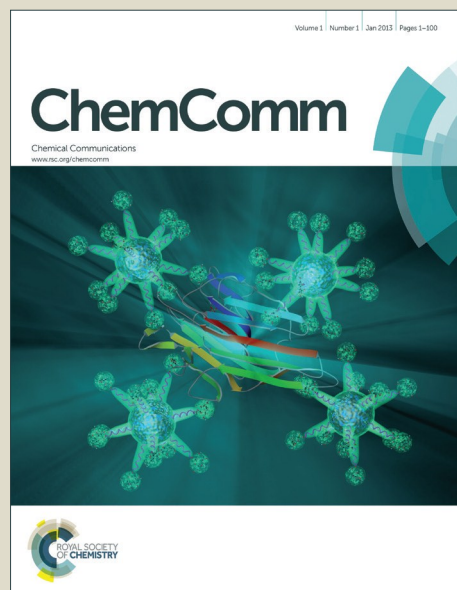


ChemComm

Accepted Manuscript



This is an Accepted Manuscript, which has been through the Royal Society of Chemistry peer review process and has been accepted for publication.

Accepted Manuscripts are published online shortly after acceptance, before technical editing, formatting and proof reading. Using this free service, authors can make their results available to the community, in citable form, before we publish the edited article. We will replace this Accepted Manuscript with the edited and formatted Advance Article as soon as it is available.

You can find more information about Accepted Manuscripts in the [Information for Authors](#).

Please note that technical editing may introduce minor changes to the text and/or graphics, which may alter content. The journal's standard [Terms & Conditions](#) and the [Ethical guidelines](#) still apply. In no event shall the Royal Society of Chemistry be held responsible for any errors or omissions in this Accepted Manuscript or any consequences arising from the use of any information it contains.



COMMUNICATION

A novel p-LaFeO₃/n-Ag₃PO₄ heterojunction photocatalyst for phenol degradation under visible light irradiation

Received 00th January 20xx,
Accepted 00th January 20xx

Jun Yang,^a Ruisheng Hu,^{*a} Wanwan Meng,^a and Yanfei Du^a

DOI: 10.1039/x0xx00000x

www.rsc.org/

A novel heterojunction photocatalyst p-LaFeO₃/n-Ag₃PO₄ has been prepared via a facile in-situ precipitation method. It exhibits higher activity than individual Ag₃PO₄ and LaFeO₃ in degradation of phenol. The excellent activity is mainly attributed to its more effective separation of electron-hole pairs.

In recent years, the problem of environmental deterioration, especially water contamination is becoming increasingly serious, semiconductor-based photocatalysis as a promising avenue has gained wide attention in the contemporary research because of its high efficiency, environmental friendliness and good cost-effect.¹ At present, the modification of a single semiconductor photocatalyst is focus on doping, which includes metal ion doping,² nonmetal ion doping,³ metal and nonmetal ion co-doping.⁴ For the method of doping modification, the photocatalytic activity is improved by increasing the oxygen defect on the photocatalyst surface. However, it has little effect on the effective separation of the photogenerated electron-hole pairs.⁵ The construction of heterojunction photocatalysts not only can effectively control the energy band structure, greatly reduce the recombination of photogenerated electrons and holes, but also can improve the stability and photocatalytic performance of the single photocatalyst.

Ag₃PO₄ as a new type of visible-light-driven photocatalyst has caused researchers' widespread concern on water splitting and photodegradation of organic contaminant.^{6,7} As is known to all, Ag₃PO₄ is a kind of n-type semiconductor,⁸ which can absorb the solar light with wavelength less than 520 nm. But the stability of the silver phosphate is poor. It has a certain solubility (0.02g/L) in aqueous solution, which makes it prone to photo-corrosion in the photocatalytic process (4Ag₃PO₄ + 6H₂O + 12h⁺ + 12e⁻ → 12Ag⁰ + 4H₃PO₄ + 3O₂).⁹ Therefore, the construction of heterojunction composites based on Ag₃PO₄ to

improve its stability has caused researchers' attention. The modification of Ag₃PO₄ by constructing n-n heterojunction has been reported, such as Ag₃PO₄/TiO₂,¹⁰ Ag₃PO₄/BiVO₄,¹¹ Ag₃PO₄/CeO₂,¹² and etc. But so far the modification of p-n heterojunction based on Ag₃PO₄ is scarcely reported. The p-n-type heterostructure exists the built-in electrical potential in the space charge region from n-type side to the p-type side, which can direct the electrons and holes to quickly migrate at the opposite direction, and this is helpful for more effective separation and longer lifetime of electron-hole pairs.¹³

To date, n-type perovskite semiconductor photocatalysts have been widely studied, such as SrTiO₃,¹⁴ NaNbO₃,¹⁵ NaTaO₃,¹⁶ and etc. However, the band gaps of these n-type perovskite semiconductors are relatively wide, which limits their ability to capture the visible light. LaFeO₃ as a kind of p-type semiconductor is a potential photocatalyst, which can be driven by visible light because of the narrow band gap.¹⁷ Currently, the research on LaFeO₃ is mainly focus on the preparation methods,¹⁸ and metal and nonmetal doping modification to improve the photocatalytic activity.¹⁹ But the downside of these approaches is the low separation efficiency of photo-generated electrons and holes. Constructing a kind of p-n-type heterojunction composite maybe can improve this disadvantage. To the best of our knowledge, the coupled photocatalyst p-LaFeO₃/n-Ag₃PO₄ for degradation of phenol has not been reported. Herein, in this work, a new composite photocatalyst p-LaFeO₃/n-Ag₃PO₄ is designed via an in-situ precipitation method in the silver-ammonia solution to eliminate phenol under visible light irradiation.

The phase composition of the samples is examined by XRD as shown in Fig. 1. All the detectable peaks in Fig. 1 (a) can be accurately indexed to the orthorhombic phase of LaFeO₃ (JCPDS card, no. 37-1493). The characteristic peaks of Ag₃PO₄ (Fig. 1f) are in good accordance with the cubic phase of Ag₃PO₄ (JCPDS card, no. 06-0505). And the Ag₃PO₄/LaFeO₃ hybrids with different mass fraction of Ag₃PO₄ exhibit a coexistence of Ag₃PO₄ and LaFeO₃ phases as shown in Fig. 1 (b), (c), (d) and (e). Peaks related to other materials are not detected, indicating that Ag₃PO₄ does not react with the LaFeO₃. Furthermore, for

^a Key Laboratory of Chemistry and Physics of Rare Earth Materials, College of Chemistry and Chemical Engineering, Inner Mongolia University, Hohhot, Inner Mongolia 010021, PR China. E-mail: cehrs@imu.edu.cn;

† Electronic Supplementary Information (ESI) available: Experimental details, characterization, and Fig. S1 to S6. See DOI: 10.1039/x0xx00000x

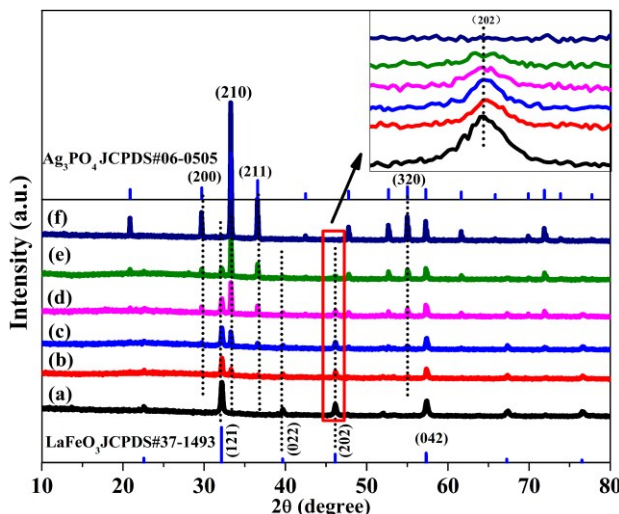


Fig. 1 XRD patterns of (a) LaFeO_3 , (b) $\text{LaFeO}_3/\text{Ag}_3\text{PO}_4$ -20%, (c) $\text{LaFeO}_3/\text{Ag}_3\text{PO}_4$ -40%, (d) $\text{LaFeO}_3/\text{Ag}_3\text{PO}_4$ -60%, (e) $\text{LaFeO}_3/\text{Ag}_3\text{PO}_4$ -80% (f) Ag_3PO_4 ($\text{LaFeO}_3/\text{Ag}_3\text{PO}_4$ -X, X represents the mass fraction of Ag_3PO_4 in the composite system.)

all the composites, the intensities of the diffraction peaks of Ag_3PO_4 increase with its increasing mass fraction, whereas those of LaFeO_3 decrease simultaneously.

The detailed characterization of the morphologies and heterojunction features of the photocatalysts is based on SEM and TEM. Fig. 2 (a) shows the SEM image of bare Ag_3PO_4 . It is clear that pure Ag_3PO_4 exhibits polyhedron morphology with an average edge length of about 2–4 μm and average diameter of about 450 nm. Fig. 2 (b) gives an overview of the SEM image of bare LaFeO_3 which exhibits irregular particles with a diameter of 60–160 nm. It can be seen that the particles are much smaller than those of pure Ag_3PO_4 . Furthermore, the morphology of the composite $\text{LaFeO}_3/\text{Ag}_3\text{PO}_4$ -60% is shown in Fig. 2c and Fig. 2d. It is clear that LaFeO_3 particles are formed on the surface of Ag_3PO_4 , and the two phases are obviously intimately intermixed. The HRTEM images of $\text{LaFeO}_3/\text{Ag}_3\text{PO}_4$ -60% composite are displayed in Fig. 2e and Fig. 2f. Obviously, two different kinds of lattice fringes can be observed. One of the fringe intervals is 0.24 nm, which matches the interplanar spacing of (201) plane for LaFeO_3 . The other one is 0.26 nm, which assigns to the (210) crystallographic plane of Ag_3PO_4 .²⁰ Based on the above results, it can be deduced that the heterojunction structure is formed between the two phases.

The XPS spectra of LaFeO_3 , Ag_3PO_4 and $\text{LaFeO}_3/\text{Ag}_3\text{PO}_4$ -60% composite are further applied to investigate the chemical composition and surface state (Fig. S1, ESI†). The results (provided in the ESI†) further demonstrate the coexistence of LaFeO_3 and Ag_3PO_4 . And it can be observed that both hydroxyl oxygen and adsorbed oxygen content of the heterojunction composite are higher than the individual LaFeO_3 and Ag_3PO_4 . According to the reported literature,²¹ hydroxyl oxygen and adsorbed oxygen can produce a mass of hydroxyl radicals and hydrogen peroxide, which have the strong oxidation property. Moreover, compared with the pure Ag_3PO_4 , the binding energy of phosphorus in $\text{LaFeO}_3/\text{Ag}_3\text{PO}_4$ -60% composite undergoes a chemical shift, indicating the strong interaction between

LaFeO_3 and Ag_3PO_4 , which implies the existence of electron transfer and chemical bonds between the two components.²²

Fig. 3 (a) shows the UV-vis diffuse reflectance spectra of the $\text{LaFeO}_3/\text{Ag}_3\text{PO}_4$ composites together with those of bare LaFeO_3 and Ag_3PO_4 . It can be seen that the absorption edge of bare LaFeO_3 at about 570 nm, and bare Ag_3PO_4 has an absorption edge at about 530 nm. For $\text{LaFeO}_3/\text{Ag}_3\text{PO}_4$ heterostructures, it is obvious that the ability of visible light absorption is enhanced and the $\text{LaFeO}_3/\text{Ag}_3\text{PO}_4$ -60% composite exhibits the strongest absorption intensity. Fig. S2 (ESI†) shows the plot of $(\text{Ahv})^2$ vs. $h\nu$, the band gaps of Ag_3PO_4 and LaFeO_3 are respectively estimated to be 2.35 eV and 2.09 eV. The band gap energy of $\text{LaFeO}_3/\text{Ag}_3\text{PO}_4$ -60% is calculated to be 2.13 eV, which is obviously narrower than that of pure Ag_3PO_4 . Thus it can be concluded that the heterojunction composite is more easily excited by visible light and the utilization ratio of visible light is enhanced.

In order to explore the recombination of photo-generated carriers, the photocurrent test was carried out. Fig. 3 (b) shows the photocurrent-voltage curves for LaFeO_3 , Ag_3PO_4 and $\text{LaFeO}_3/\text{Ag}_3\text{PO}_4$ -60% composite under several on/off visible-light irradiation cycles. In comparison with pure LaFeO_3 and Ag_3PO_4 , $\text{LaFeO}_3/\text{Ag}_3\text{PO}_4$ -60% composite shows an obviously larger photocurrent under visible light irradiation ($\lambda > 420$ nm). The intensity of the photocurrent is an important parameter to evaluate the photocatalytic performance of catalyst. Higher photocurrent means lower recombination of electron-hole pairs and more visible light absorption.²³ Especially that photocatalytic reaction involves a series of redox reactions, in some degree, higher photocurrent also reveals an improved redox property of the catalyst.²⁴

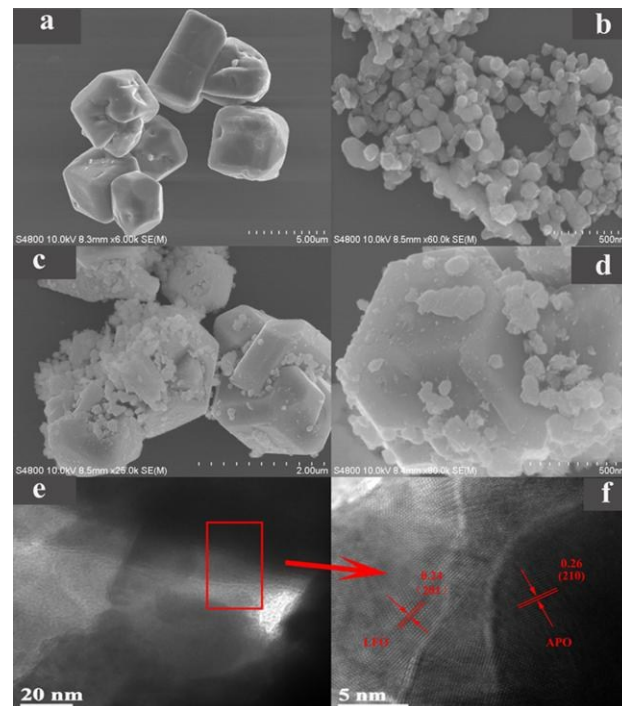


Fig. 2 SEM images of (a) Ag_3PO_4 , (b) LaFeO_3 , and (c, d) $\text{LaFeO}_3/\text{Ag}_3\text{PO}_4$ composites (mass ratio = 4:6). And TEM images of (e, f) $\text{LaFeO}_3/\text{Ag}_3\text{PO}_4$ (mass ratio = 4:6)

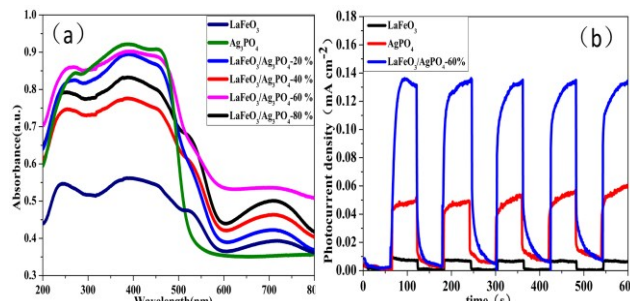


Fig.3 (a) UV-vis diffuse reflectance spectra of LaFeO₃, Ag₃PO₄ and LaFeO₃/Ag₃PO₄ (b) Photocurrents of LaFeO₃, Ag₃PO₄, and LaFeO₃/Ag₃PO₄-60% under the irradiation of visible light.

The photocatalytic activity was investigated by phenol degradation under the visible light irradiation as shown in Fig.4 (a). It obviously can be seen that the photocatalytic performance of LaFeO₃ is enhanced by the incorporation of an appropriate amount of Ag₃PO₄. Among all of the samples, LaFeO₃/Ag₃PO₄-60% composite exhibits the best activity, whose degradation rates is 3.50 times of single Ag₃PO₄ and 5.81 times of single LaFeO₃, respectively. In order to study the effect of the intermediate products on the absorbance of phenol, the UV absorbance spectra of phenol are given as shown in Fig.4 (b). The maximum absorption peak of phenol can be seen at 270 nm and it does not shift. What's more, the maximum absorbance value gradually decreases from 0 min to 120 min, which indicates that the concentration of phenol decreases with irradiation time. The kinetic study was also carried out as shown in Fig. S3 (ESI†). LaFeO₃/Ag₃PO₄-60% composite shows the maximal degradation rate constant (0.02036 min⁻¹), which is 15.19 times of bare LaFeO₃ and 8.02 times of pure Ag₃PO₄. Thus, it can be deduced that constructing the p-n heterojunction LaFeO₃/Ag₃PO₄ can greatly improve the photocatalytic performance of the individual catalyst. The higher chemical oxygen demand (COD) removal rate indicates the higher organic matter mineralization rate during the photocatalytic degradation progress. Fig.S4 (ESI†) reveals the results of the COD removal rate, it can be seen that the composite LaFeO₃/Ag₃PO₄-60% exhibits the highest COD removal rate, which is much higher than the single LaFeO₃ and Ag₃PO₄. The stability of LaFeO₃/Ag₃PO₄-60% composite and fresh Ag₃PO₄ was investigated as shown in Fig.S5 (ESI†). As can be seen in the ESI file, the composite LaFeO₃/Ag₃PO₄-60% exhibits much more higher stability than the individual Ag₃PO₄.

The position of conduction band (CB) and valence band (VB) of a semiconductor is one of the important factors that affect the photocatalytic activity. Although it is difficult to determine the potentials by experiment, the potentials of the conduction band and valence band edges can be obtained according to the Mulliken electronegativity theory as shown in Eq.S1 and Eq.S2 (ESI†). The calculated rough conduction band and valence band edge potentials can be obtained as follows: LaFeO₃: E_{CB}=0.025 eV, E_{VB}=2.115 eV; Ag₃PO₄: E_{CB}=0.285 eV, E_{VB}=2.635 eV. It is obvious that the CB and VB edge potential positions of LaFeO₃ are both more negative than that of Ag₃PO₄. LaFeO₃ in the heterojunction structure would absorb photons to

generate electron-hole pairs under visible light irradiation. Subsequently, owing to the existence of the built-in electrical potential in the space charge region with the direction from n-type Ag₃PO₄ to the p-type LaFeO₃, the photo-generated electrons on the CB bottom of LaFeO₃ would easily transfer to the CB of Ag₃PO₄ via the well connected interface, and meanwhile holes on the VB of Ag₃PO₄ will diffuse into the VB of LaFeO₃. In this way, the effective separation of the electron-hole pairs is accomplished, which can be seen in fig. 5. In order to confirm the above discussion, the photoluminescence spectra were further recorded as shown in Fig.S3 (ESI†). To further investigate the separation and transfer process of photo-induced charges, SPV measurement was carried out and the results were shown in the ESI file.

In order to explore whether the specific surface area could make a difference in the photocatalytic performance, N₂ adsorption-desorption measurement was carried out. The results (Fig.S6, ESI†) indicate that there are only small differences among the surface area values of LaFeO₃/Ag₃PO₄ composites. It can be speculated that the different photocatalytic activities of the samples could not be determined by the BET surface areas.

In the photocatalytic process, active species mainly involve hole (h⁺), hydroxyl radical (OH) and superoxide radical (O₂^{•-}). So what kind of active species is the key in the photo-degradation reaction? The free radical capture experiments were conducted by adding different active species scavengers using phenol photodegradation as the model reaction. The experimental details are shown in ESI file. The result as shown in Fig.S6 (ESI†) gives evidence that the degradation of phenol is dominated by the oxidation reaction of hydroxyl radical and the direct hole oxidation.

The generation of active species is closely relevant to the potential energy of the conduction band and valence band of semiconductors. The CB edge potential of Ag₃PO₄ is 0.285 eV (vs. NHE), which is more positive than the standard redox potential E^θ (O₂/O₂^{•-}) (-0.33 eV vs. NHE),²⁵ indicating that the electrons at CB of Ag₃PO₄ cannot reduce O₂ to O₂^{•-}. This is consistent with the result of the free radical capture test, which is also proved that superoxide radicals are not the

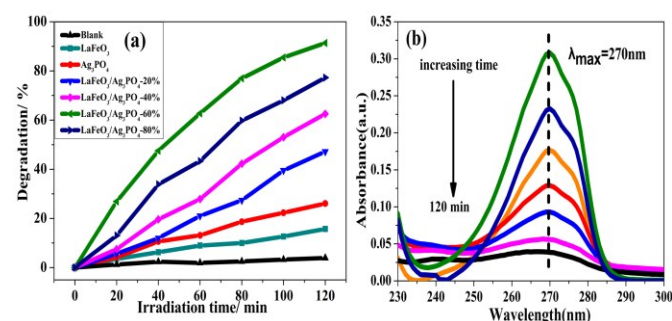


Fig.4 (a) Photocatalytic activities of LaFeO₃, Ag₃PO₄, LaFeO₃/Ag₃PO₄ composites, and without catalyst (blank experiment) under visible light irradiation; (b) The UV absorbance of the phenol with time (from 0 min to 120 min).

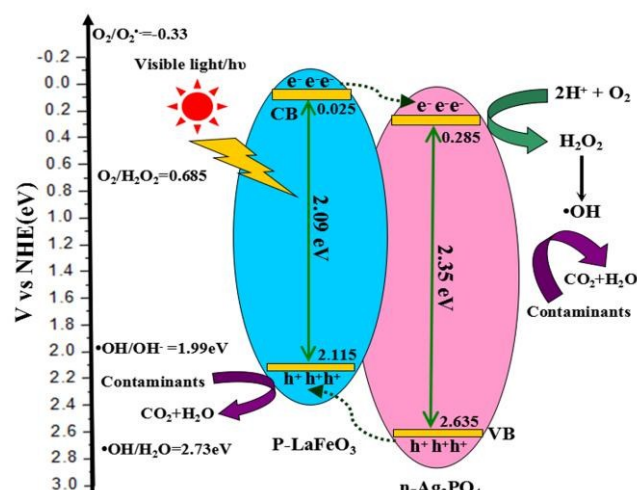
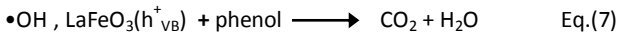
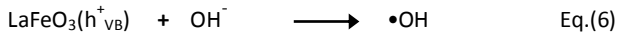
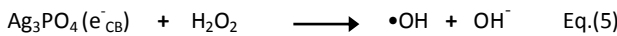
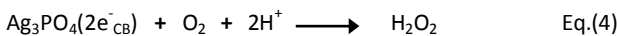


Fig.5 Schematic diagram of electron-hole pairs' separation process and the photocatalytic process .

reactive species. However, the CB edge potential of Ag_3PO_4 is more negative than the standard redox potential E^\ominus ($\text{O}_2/\text{H}_2\text{O}_2$) (0.685 eV vs. NHE),²⁵ suggesting that oxygen adsorbed on the surface of the composite semiconductor can react with two electrons to form H_2O_2 as shown in Eq.(4), and subsequently H_2O_2 can combine with one electron to further form OH as described in Eq. (5). And that OH shows strong oxidation characteristic to participate in the photocatalytic reaction as shown in Eq. (7). Furthermore, the VB edge potential of LaFeO_3 (2.115 eV vs. NHE) is more positive than the standard redox potential of E^\ominus (OH/OH^-) (1.99 eV vs. NHE),²¹ suggesting that the accumulated holes on the VB of LaFeO_3 can oxidize OH^- to form OH as shown in Eq. (6) and the results of the XPS show that a large amount of hydroxyl oxygen exist on the surface of the composite, which provides a reliable basis for the inference. Part of the holes may be directly involved in the oxidation of organic compounds according to the above free radicals capture experiment. In a word, hydroxyl free radicals play the primary role in the photocatalytic degradation of phenol. Based on the above discussion, the progress of phenol degradation is as follows:



In summary, a novel p-n heterojunction photocatalyst $\text{LaFeO}_3/\text{Ag}_3\text{PO}_4$ was successfully synthesized via an in-situ precipitation method. Compared with the individual Ag_3PO_4 and LaFeO_3 , the composite photocatalysts exhibit much higher photocatalytic performance and stability for phenol degradation under visible light irradiation. The superior

photocatalytic activity of the heterojunction photocatalyst is mainly attributed to the existence of the built-in electric field, which can promote the separation of photogenerated electron and hole pairs effectively.

This work is supported by the National Natural Science Foundation of China (No.21166015).

Notes and references

- A. Kubacka, M. Fernández-García and G. Colón, *Chem. Rev.*, 2012, **112**, 1555.
- G. Cappelletti, V. Pifferi, S. Mostoni, L. Falciola, C. Di Bari, F. Spadavecchia, D. Meroni, E. Davoli and S. Ardizzone, *Chem. Commun.*, 2015, **51**, 10459.
- W. K. Ho, J. C. Yu and S. C. Lee, *Chem. Commun.*, 2006, **10**, 1115.
- X. Lan, L. Z. Wang, B. Y. Zhang, B. Z. Tian and J. L. Zhang, *Catal. Today*, 2014, **224**, 163.
- H. J. Li, Y. Zhou, W. G. Tu, J. H. Ye and Z. G. Zou, *Adv. Funct. Mater.*, 2015, **25**, 998.
- Y. P. Bi, H. Y. Hu, S. X. OuYang, G. X. Lu, J. Y. Cao and J. H. Ye, *Chem. Commun.*, 2012, **48**, 3748.
- X. Y. Guo, C. F. Chen, S. Y. Yin, L. J. Huang and W. P. Qin, *J. Alloys Compd.*, 2015, **619**, 293.
- Z. G. Yi, J. H. Ye, N. Kikugawa, T. Kako, S. X. Ouyang, H. Stuart-Williams, H. Yang, J. Y. Cao, W. J. Luo, Z. S. Li, Y. Liu and R. L. Withers, *Nat. Mater.*, 2010, **9**, 559.
- H. Wang, Y. Bai, J. Yang, X. Lang, J. Li and L. Guo, *Chem. Eur. J.*, 2012, **18**, 5524.
- C. Tang, E. Liu, J. Fan, X. Hu, L. Kang and J. Wan, *Ceram. Int.*, 2014, **40**, 15447.
- C. J. Li, P. Zhang, R. Lv, J. W. Lu, T. Wang, S. P. Wang, H. F. Wang and J. L. Gong, *Small*, 2013, **9**, 3951.
- Z. M. Yang, G. F. Huang, W. Q. Huang, J. M. Wei, X. G. Yan, Y. Y. Liu, C. Jiao, Z. Wan and A. L. Pan, *J. Mater. Chem. A*, 2014, **2**, 1750.
- H. L. Wang, L. S. Zhang, Z. G. Chen, J. Q. Hu, S. J. Li, Z. H. Wang, J. S. Liu and X. C. Wang, *Chem. Soc. Rev.*, 2014, **43**, 5234.
- F. Zou, Z. Jiang, X. Q. Qin, Y. X. Zhao, L. Y. Jiang, J. F. Zhi, T. C. Xiao and P. P. Edwards, *Chem. Commun.*, 2012, **48**, 8514.
- S. Kumar, S. Khancharanani, M. Thirumal and A. K. Ganguli, *ACS Appl. Mater. Interfaces*, 2014, **6**, 13221.
- P. Kanhere, P. Shenai, S. Chakraborty, R. Ahuja, J. W. Zheng and Z. Chen, *Phys. Chem. Chem. Phys.*, 2014, **16**, 16085.
- Q. Yu, X. G. Meng, T. Wang, P. Li, L. Q. Liu, K. Chang, G. G. Liu and J. H. Ye, *Chem. Commun.*, 2015, **51**, 3630.
- P. S. Tang, Y. Tong, H. F. Chen, F. Cao and G. X. Pan, *Current Applied Physics*, 2013, **13**, 340.
- Z. X. Wei, Y. Wang, J. P. Liu, C. M. Xiao and W. W. Zeng, *Mater. Chem. Phys.*, 2012, **136**, 755.
- S. S. Patil, M. S. Tamboli, V. G. Deonikar, G. G. Umarji, J. D. Ambekar, M. V. Kulkarni, S. S. Kolekar, B. B. Kale and D. R. Patil, *Dalton Trans.*, 2015, **44**, 20426.
- T. T. Wang, J. Y. Lang, Y. J. Zhao, Y. G. Su, Y. X. Zhao and X. J. Wang, *CrystEngComm*, 2015, **17**, 6651.
- F. T. Li, Y. Zhao, Q. Wang, X. J. Wang, Y. J. Hao, R. H. Liu and D. S. Zhao, *J. Hazard. Mater.*, 2015, **283**, 371.
- C. Z. Luo, D. L. Li, W. H. Wu, C. Z. Yu, W. P. Li and C. X. Pan, *Appl. Catal., B*, 2015, **166-167**, 217.
- J. Y. Lang, C. Y. Li, S. W. Wang, J. J. Lv, Y. G. Su, X. J. Wang, and G. S. Li, *ACS Appl. Mater. Interfaces*, 2015, **7**, 13905.
- J. J. Guo, S. X. Ouyang, H. Zhou, T. Kako and J. H. Ye, *J. Phys. Chem. C*, 2013, **117**, 17716.